Anal. Chem. **2002,** *74,* 1149−1156

Biomolecular Recognition on Well-Characterized Beads Packed in Microfluidic Channels

Tione Buranda,*,† Jinman Huang,‡ Victor H. Perez-Luna,§ Brett Schreyer,|| Larry A. Sklar,*,†,⊥ and Gabriel P. Lopez*,||

Cancer Center and Department of Pathology, University of New Mexico School of Medicine, NSF Center for Micro-Engineered Materials, and Chemical and Nuclear Engineering and Department of Chemistry, University of New Mexico, Albuquerque, New Mexico 87131, Bio-sciences Division and National Flow Cytometry Resource, Los Alamos National Laboratories, Los Alamos, New Mexico 87545, and Department of Chemical and Environmental Engineering, Illinois Institute of Technology, Chicago, Illinois 60616

We describe a new approach for the analysis of biomolecular recognition in microfluidic channels. The method involves real-time detection of soluble molecules binding to receptor-bearing microspheres, sequestered in affinity column format inside a microfluidic channel. Identification and quantitation of analytes occurs via direct fluorescence measurements or fluorescence resonance energy transfer (FRET). We establish a model system that detects the FLAG epitope. The assay can potentially detect subfemtomole quantities of antibody with a high signal-to-noise ratio and a large dynamic range spanning nearly 4 orders of magnitude in analyte concentration in microliter-to-submicroliter volumes of analyte fluid. Kinetic and equilibrium constants for the reaction of this receptor−ligand pair are obtained through modeling of kinetic responses of the affinity microcolumn and are consistent with those obtained by flow cytometry. Because of the correlation between kinetic and equilibrium data obtained for the microcolumns, quantitative analysis can be done prior to the steady-state end point of the recognition reaction. This method has the promise of combining the utility of affinity chromatography with the advantage of direct, quantitative, and real-time analysis and the cost-effectiveness of microanalytical devices. The approach has the potential to be generalized to a host of bioaffinity assay methods including analysis of protein complexes and molecular assembly and microsystem-based multianalyte determinations.

The analysis of macromolecular interactions, assemblies, and their function is an essential component of biomedical research. This effort is driven by the need to identify diagnostic or therapeutic targets of disease, biological interactions in proteomics for protein−protein as well as small-molecule interactions, and biosensing.[1−10] Important progress in the development of new technologies for biomolecular analysis has been made, in particular, in the area of microfluidic devices.[11] Microfluidic devices generally consume submicroliter quantities of sample and are thus well suited for use when the required reagents are scarce or expensive. Because of their size, microfluidic devices operate in a regime where small Reynolds numbers[12] govern the delivery of fluid samples. Fast mixing of reagents is one of several issues that present a major challenge to the operation of microfluidic devices. Due to negligible inertial forces,[12] mixing of solutes in microchannels is generally driven by diffusion alone[13,14] and is therefore slow and often ineffective even at micrometer scales. The full potential of microdevices is yet to be realized due to unresolved issues associated with factors such as fluid transport and quantitative analysis (chemical reaction, product separation, identification) of molecular interactions.

A prevailing trend in the development of bioanalytical assays is the display of biochemical reagents on synthetic microbeads.[15−25]

* Corresponding authors: (T.B.) buranda@unm.edu; (L.A.S.) lsklar@salud.unm.edu; (G.P.L.) gplopez@unm.edu.

† Cancer Center and Department of Pathology, University of New Mexico School of Medicine.

‡ NSF Center for Micro-Engineered Materials, University of New Mexico.

§ Illinois Institute of Technology.

|| Chemical and Nuclear Engineering and Department of Chemistry, University of New Mexico.

⊥ Los Alamos National Laboratories.

(1) Borman, S. *Chem. Eng. News* **2000**, *78* (July 31), 31−37.
(2) Paddle, B. M. *Biosens, Bioelectron.* **1996**, *11*, 1079−1113.
(3) Piervincenzi, R. T.; Reichert, W. M.; Hellinga, H. W. *Biosens, Bioelectron.* **1998**, *13*, 305−312.
(4) Vijayendran, R. A.; Leckband, D. E. *Anal. Chem.* **2001**, *73*, 471−480.
(5) Walt, D. R.; Dickinson, T.; White, J.; Kauer, J.; Johnson, S.; Engelhardt, H.; Sutter, J.; Jurs, P. *Biosens, Bioelectron.* **1998**, *13*, 697−699.
(6) Wang, J. *Anal. Chem.* **1999**, *71*, R328−R332.
(7) Wang, J. *J. Pharm. Biomed. Anal.* **1999**, *19*, 47−53.
(8) Cornell, B. A.; Braach-Maksvytis, V. L. B.; King, L. G.; Osman, P. D. J.; Raguse, B.; Wieczorek, L.; Pace, R. J. *Nature* **1997**, *387*, 580−583.
(9) Dodson, J. M.; Feldstein, M. J.; Leatzow, D. M.; Flack, L. K.; Golden, J. P.; Ligler, F. S. *Anal. Chem.* **2001**, *73*, 3776−3780.
(10) Wortberg, M.; Orban, R. R.; Cammann, K. In *Handbook of Biosensor and Electronic Noses: Medicine, Food and the Environment*; Kress-Rogers, E., Ed.; CRC Press: Boca Raton FL, 1997.
(11) Quake, S. R.; Scherer, A. *Science* **2000**, *290*, 1536−1540.
(12) Purcell, E. M. *Am. J. Phys.* **1977**, *45*, 3−11.
(13) Brody, J. P.; Yager, P.; Goldstein, R. E.; Austin, R. H. *Biophys. J.* **1996**, *71*, 3430−3441.
(14) Knight, J. B.; Ashvin, V.; Brody, J. P.; Austin, R. H. *Phys. Rev. Lett.* **1998**, *80*, 3863−3866.
(15) Bangs, L. B. *Pure Appl. Chem.* **1996**, *68*, 1873−1879.
(16) Goodey, A.; Lavigne, J. J.; Savoy, S. M.; Rodriguez, M. D.; Curey, T.; Tsao, A.; Simmons, G.; Wright, J.; Yoo, S. J.; Sohn, Y.; Anslyn, E. V.; Shear, J. B.; Neikirk, D. P.; McDevitt, J. T. *J. Am. Chem. Soc.* **2001**, *123*, 2559−2570.
(17) Lavigne, J. J.; Savoy, S.; Clevenger, M. B.; Ritchie, J. E.; McDoniel, B.; Yoo, S. J.; Anslyn, E. V.; McDevitt, J. T.; Shear, J. B.; Neikirk, D. *J. Am. Chem. Soc.* **1998**, *120*, 6429−6430.
(18) Marchenko, S. B.; Zhdanov, A. A.; Gritskova, I. A.; Zaitsev, S. Y. *Polym. Sci. Ser. A* **2001**, *43*, 273−277.

10.1021/ac0109624 CCC: $22.00 © 2002 American Chemical Society
Published on Web 02/02/2002

Important progress has been made in the incorporation of microbeads in sensor arrays whose functions are analogous to natural sensory functions of smell[5,26] and taste.[16,17]

Concurrent with these developments, progress has been made in molecular approaches to incorporating fluorescent tags into proteins, as well as bead-based surface chemistries and calibration methods. These advances allow the quantitative study of these molecular interactions by flow cytometry.[27,28] For several years we have participated in this trend and thus have extensive experience in developing biosensing strategies that display fluorescently labeled receptors and ligands on microbeads.[28−30] Through this endeavor, we have shown how molecular assemblies on beads can be analyzed in a quantitative fashion by flow cytometry.

In this study, we have used beads calibrated with flow cytometry[28] as platforms in an affinity microcolumn format for the quantitative detection of analytes in microfluidic channels (Figure 1A). There are several advantages to this approach: (a**)** Molecular assemblies for the assay are created outside the channel on beads and characterized with flow cytometry. (b) Uniform populations of beads may be ensured through rapid cytometric sorting. (c) Beads present a larger surface area for the display of receptors than flat surfaces. This is a clear improvement over those techniques that rely on the micropatterning of reactive molecules on flat surfaces.[31] Mixing of solutes in laminar flows occurs by diffusion with a typical diffusion coefficient for biomolecules on the order of $\leq 10^{-7}$ cm^2/s. Thus, mixing by diffusion is slow. Rapid mixing in the microcolumn is achieved because the distance that must be covered by diffusion is limited to the (small) interstitial space between the closely packed receptor-bearing beads. Analytes are captured in flow-through format and as such each bead can act as a local concentrator of analytes.[20,32]

Epitope tagging is a widely practiced technique used to purify and study structure and functional properties of proteins.[33−36] The

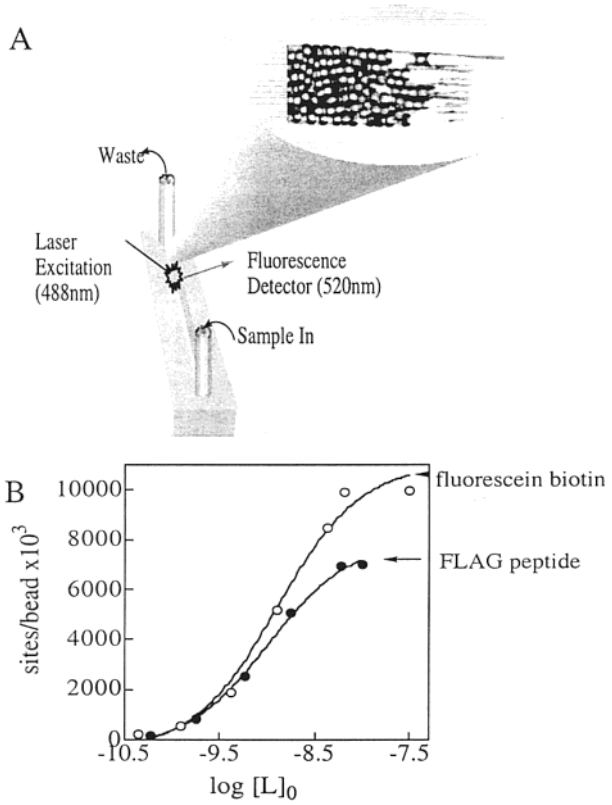

Figure 1. (A) Schematic of a microfluidic apparatus showing the configuration in which sample was delivered and fluorescence measurements taken with a spectrofluorometer. Elastomeric silicone microchannel, mounted on glass slide with two openings for sample delivery and egress. The microchannel is 250 μm wide, 50 μm deep, and 3 cm long. Patterned features (inset) 20 μm apart, act as filters for holding 30-μm borosilicate beads. Thirty thousand, 6.2-μm streptavidin-coated beads form a ~600-μm-long affinity microcolumn. Site occupancies were determined from binding curves shown in (B). (B) Equilibrium binding curves for fluorescein biotin and FLAG peptide. The sites/bead were determined from centrifugation assays, and L_0 refers to the initial concentrations of fluorescein biotin or biotinylated FLAG peptide. The full analysis of these equilibrium binding assays has been described elsewhere.[28,39]

FLAG system is a commonly used epitope tag that relies on the octapeptide DYKDDDDK, with readily available monoclonal antibodies.[34−36] This system is an ideal model for the development of generalizable assays for proteins with known epitopes. This report describes the detection of analytes and the determination of kinetic and equilibrium constants of binding between fluorescently labeled FLAG peptides and anti-FLAG antibodies in microchannels. Samples of Texas Red-labeled anti-FLAG monoclonal antibodies (TR-M1 mAbs) were pumped through an affinity microcolumn with fluorescein-tagged FLAG peptides on beads with known site densities. The interaction between the TR-M1 mAbs and beads was monitored via fluorescence resonance energy transfer (FRET).[37] Monitoring the amount of ligand/receptor complexes formed at a wide range of concentrations of TR-M1 mAbs gave access to the kinetic and equilibrium parameters of the antibody−peptide reaction. The data from affinity microcolumns were compared to data measured in a conventional flow cytometer assay.

(19) Weimer, B. C.; Walsh, M. K.; Wang, X. W. *J. Biochem. Biophys. Methods* **2000**, *45*, 211−219.
(20) Oleschuk, R. D.; ShultzLockyear, L. L.; Ning, Y. B.; Harrison, D. J. *Anal. Chem.* **2000**, *72*, 585−590.
(21) Sato, K.; Tokeshi, M.; Odake, T.; Kimura, H.; Ooi, T.; Nakao, M.; Kitamori, T. *Anal. Chem.* **2000**, *72*, 1144−1147.
(22) Sato, K.; Tokeshi, M.; Kimura, H.; Kitamori, T. *Anal. Chem.* **2001**, *73*, 1213−1218.
(23) Andersson, H.; vanderWijngaart, W.; Enoksson, P.; Stemme, G. *Sens. Actuators, B* **2000**, *67*, 203−208.
(24) Andersson, H.; Jonsson, C.; Moberg, C.; Stemme, G. *Electrophoresis* **2001**, *22*, 3876−3882.
(25) Andersson, H.; van der Wijngaart, W.; Stemme, G. *Electrophoresis* **2001**, *22*, 249−257.
(26) Albert, K. J.; Lewis, N. S.; Schauer, C. L.; Sotzing, G. A.; Stitzel, S. E.; Vaid, T. P.; Walt, D. R. *Chem. Rev.* **2000**, *100*, 2595−2626.
(27) Nolan, J.; Chambers, J. D.; Sklar, L. A. In *Cytometry Approaches to Cellular Analysis*; Babcock, G. P. R., Ed.; Wiley-Liss: New York, 1998.
(28) Buranda, T.; Jones, G.; Nolan, J.; Keij, J.; Lopez, G. P.; Sklar, L. A. *J. Phys. Chem. B* **1999**, *103*, 3399−3410.
(29) Nolan, J. P.; Sklar, L. A. *Nat. Biotechnol.* **1998**, *16*, 633−638.
(30) Nolan, J. P.; Lauer, S.; Prossnitz, E. R.; Sklar, L. A. *Drug Discovery Today* **1998**, *4*, 178−189.
(31) Delamarche, E.; Bernard, A.; Schmid, H.; Bietsch, A.; Michel, B.; Biebyck, H. *J. Am. Chem. Soc.* **1998**, *120*, 500−508.
(32) Hanninen, P.; Soini, A.; Meltola, N.; Soini, J.; Soukka, J.; Soini, E. *Nat. Biotechnol.* **2000**, *18*, 548−550.
(33) Cafiso, D. S. *Curr. Top. Membr.* **1999**, *48*, 197−228.
(34) Slootstra, J. W.; Kuperus, D.; Pluckthun, A.; Meloen, R. H. *Mol. Diversity* **1997**, *2*, 156−164.
(35) Brizzard, B. L.; Chubet, R. G.; Vizard, D. L. *Biotechniques* **1994**, *16*, 730−735.
(36) Knappik, A.; Pluckthun, A. *Biotechniques* **1994**, *17*, 754−761.
(37) Selvin, P. R. *Nat. Struct. Biol.* **2000**, *7*, 730−734.

The system described here reproduces the essential elements of affinity chromatography with the advantage of direct and real-time analysis and miniaturization. Furthermore, because beads can be easily configured to detect multiple analytes in the microchannel, simultaneous detection of a diverse group of analytes can be achieved by packing discrete segments of receptor bearing beads in a single affinity microsystem.[38]

RESULTS

A. Beads in Microfluidic Columns. (1) Bead Characterization. Binding data for the fluorescein biotin and FLAG peptides to streptavidin-coated beads are summarized as binding curves in Figure 1B. The magnitudes of bound sites per bead were determined from centrifugation assays.[28,39] In that analysis,[39] the affinities of fluorescein biotin and the FLAG peptide were determined to be on the order of 0.5 and 0.30 nM, respectively.[39]

(2) Affinity Microcolumns. The microfluidic channels were made from an elastomeric polymer, poly(dimethylsiloxane) (PDMS), with convenient fabrication techniques that allow for dimensions as small as 10 μm.[40,41] The prototype shown in Figure 1A is composed of a microfluidic channel, 3 cm long, with typical dimensions of 250 μm by 50 μm in breadth and depth, respectively, patterned into a PDMS elastomer adhered to a glass slide support. Surface-characterized beads (Figure 1B) were sequestered in the channels and used as platforms for the dynamic and quantitative detection of biomolecules at submicroliter volumes. Within the microchannel, obstructive features, 20 μm apart (see micrographic inset in Figure 1A) were patterned as filters to hold 30-μm beads. Beads were packed by injection of suspensions, starting with a foundation of 30-μm borosilicate beads followed by a 10-μm bead layer and the affinity microcolumn layer of 30 000, 6.2-μm streptavidin-coated beads. The streptavidin-coated beads bore biotinylated molecules of interest. The void space (interstitial bead space) within the bioactive 600-μm column is reduced to ~4.0 nL[42] and serves as the reactor vessel with an intrinsically large surface area (i.e., 30 000 beads $\times$ $4\pi r^2$).

B. Detection of Soluble Analytes in Affinity Microcolumns. (1) Detection of Native Biotin via Fluorescence Unquenching of Fluorescein Biotin. Under certain circumstances, binding of fluorescent ligands to streptavidin is characterized by the quenching of fluorescence of bound relative to free ligands.[28] Typically, this type of quenching ("ostrich quenching") occurs when the fluorophore (e.g., fluorescein) moiety of a biotinylated ligand associates with the receptor pocket adjacent to the biotin moiety-bearing site (Figure 2). Ostrich quenching is dependent on the length and structure of the ligand. We have previously shown this interaction for fluorescein biotin to be very weak ($k_{-q}/k_q \approx 0.1$)[28] and readily obstructed by native biotin.[28,43,44] Binding of fluorescein

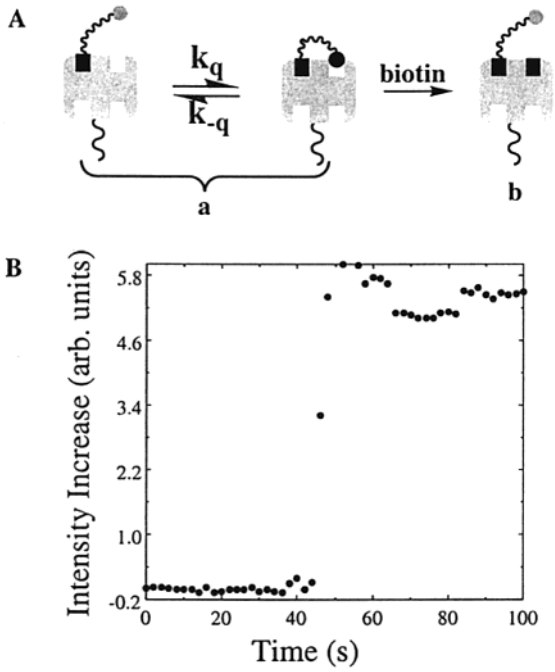

Figure 2. (A) Schematic depiction of (a) fluorescein biotin bound to streptavidin and subsequent ("ostrich") quenching interaction of fluorescein with a cis binding pocket, on the streptavidin and (b) addition of native biotin to block ostrich quenching leading to increased emission intensity by fluorophore. (B) Addition of excess native biotin to beads in channel causes a 5-fold increase in fluorescence, corresponding to the process in (b). The time resolution marks the progress of the fluid through the column of beads. The rise in the noise level associated with the signal soon after contact of native biotin with the ostrich-quenched beads is likely to be due to minor disruption of the column upon initial contact with the plug of sample.

biotin to excess soluble streptavidin results in >90% quenching of the fluorescence. Addition of native biotin recovers the original intensity under diffusion-limited kinetics. The extent of quenching and recovery on beads depends on site occupancy of the fluorescein biotin. The data in Figure 2B show a 5-fold increase in intensity of fluorescein biotin-bearing beads resulting from the injection of a 2-μL aliquot of 3 mM native biotin. The 5-fold increase in intensity was consistent with a result from a flow cytometry measurement (data not shown).

(2) Detection of Anti-FLAG Monoclonal Antibodies Via FRET. We have synthesized biotinylated and fluorescein-tagged FLAG peptides, attached them to streptavidin-coated beads (~1 $\times$ 10^6 peptides/bead), and used FRET to analyze their interaction with Texas Red-labeled anti-FLAG (TR-M1) monoclonal antibodies by flow cytometry.[39] Results from that study are compared to the analytical data collected in the affinity microcolumns described here. Several concentrations of TR-M1 mAbs were analyzed with affinity microcolumns. The results are shown in Figure 3. The binding of TR-M1 mAbs to FLAG peptide-bearing beads was monitored by FRET.

In Figure 3A, various concentrations of TR-M1 were injected into affinity columns at the rate of 1.6 nL/s. Data were normalized to the initial intensity of the beads (before passage through the column) of a 2-μL aliquot of TR-M1 mAbs. The data in Figure 3A

(38) Huang, J.; Buranda, T.; Sklar, L. A.; Lopez, G. P., work in progress.
(39) Buranda, T.; Lopez, G. P.; Simons, P.; Pastuszyn, A.; Sklar, L. A. *Anal. Biochem.* **2001**, *298*, 151−162.
(40) Duffy, D. C.; McDonald, J. C.; Schueller, O. J. A.; Whitesides, G. M. *Anal. Chem.* **1998**, *70*, 4974−4984.
(41) Duffy, D. C.; Schueller, O. J. A.; Brittain, S. T.; Whitesides, G. M. *J. Micromech. Microeng.* **1999**, *9*, 211−217.
(42) The void space of the affinity microcolumn is estimated from the difference between the volume of the microchannel occupied by the 30 000 6.2-μm beads and the volume of the empty microchannel of dimensions (250 $\times$ 50 $\times$ 600) μm^3.
(43) Buranda, T.; Lopez, G. P.; Keij, J.; Harris, R.; Sklar, L. A. *Cytometry* **1999**, *37*, 21−31.
(44) Gruber, H. J.; Marek, M.; Schindler, H.; Kaiser, K. *Bioconjugate Chem.* **1997**, *8*, 552−559.

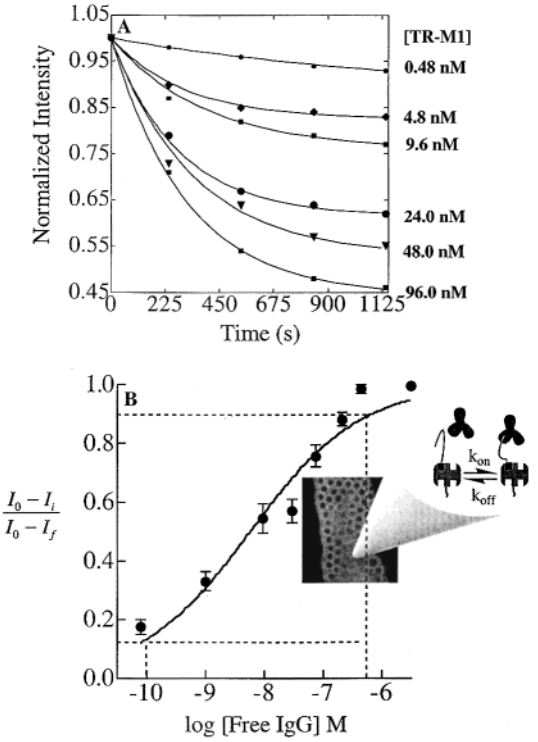

Figure 3. (A) Binding curves of 2-μL plugs of Texas-Red-labeled monoclonal anti-FLAG antibodies through affinity microcolumns of fluorescein-labeled FLAG peptide-bearing beads. The points refer to the normalized intensity readings taken during each run. The lines represent least-squares fits to the data (using eq 2) resulting in the determination of the average association and dissociation rate constants: $k_f = (9.0 \pm 6.0) \times 10^4$ M^{-1} s^{-1}, $k_b = (1.2 \pm 0.8) \times 10^{-3}$ s^{-1}. (B) Sigmoidal dose−response binding curve of TR-M1 mAbs obtained after passage through the affinity microcolumn (inset). Along the *y*-axis, I_0 is the initial intensity of beads; I_i is the intensity of beads after binding to TR-M1 mAbs, of a given concentration, *and* I_f corresponds to the intensity of beads after binding to the saturating concentration of TR-M1. Data represent three different measurements per concentration of TR-M1. The dissociation constant from the analysis is ∼10 nM. Dashed lines have been drawn at 10% and 90% analyte saturation showing a dynamic range of ∼4 orders of magnitude.

were fit to a kinetic model shown in eq 1,

$$\frac{d\Gamma_{AB}}{dt} = k_f C_0 \Gamma_A - k_b \Gamma_{AB} = \frac{D}{\delta}(C^b - C_0) \qquad (1)$$

expressed in terms of bimolecular interactions and diffusion-limited conditions.[45] C^b and C_0 represent the concentrations of antibody in the bulk and at the liquid−solid interface, respectively; Γ_{AB} is the surface concentration of FLAG peptides bound to antibodies; Γ_A is the surface concentration of unbound peptides; and k_f and k_b are the forward and reverse kinetic rate constants, respectively. D is the diffusion coefficient of the antibody and δ is the thickness of the steady-state diffusion−convection boundary layer established by fluid transport in which we assume a linear gradient in concentrations (between C^b and C_0). The parameter D/δ represents the effects of diffusive transport of analytes to

(45) Bourdillon, C.; Demaille, C.; Moiroux, J.; Saveant, J.-M. *J. Am. Chem. Soc.* **1999**, *121*, 2401−2408.

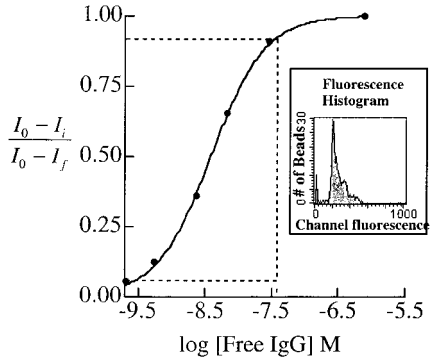

Figure 4. Binding of TR-M1 mAbs to bead-borne FLAG peptides in flow cytometry ($K_d \approx 4.0$ nM). Normalized intensities are derived from the means of fluorescence histograms (inset) of bead suspensions incubated with various concentrations of TR-M1 mAbs and normalized to bead intensity prior to exposure to TR-M1 mAbs. The dotted lines are as described in Figure 3B. The contrast is discussed in the text.

the surface receptors. The integral form of this equation is shown in eq 2 in the dimensionless formalism given by Savéant et al.[45]

$$\lambda\theta - \left(1 + \frac{\lambda}{1+\kappa}\right)\ln\left(1 - \frac{1+\kappa}{\kappa}\theta\right) = \frac{1+\kappa}{\kappa}\lambda\tau \qquad (2)$$

In this equation $\theta = \Gamma_{AB}/\Gamma^S$ (where Γ^S (= $\Gamma_{AB} + \Gamma_A$) represents the total surface concentration of FLAG peptides). The adsorption constant is, $\kappa = (k_f/k_b)C^b$, the diffusion-dependent rate of adsorption, $\lambda = (k_f\delta\Gamma^S/D)$, and the dimensionless time normalized to diffusion time, $\tau = (t/t_d)$, (where the time that characterizes the diffusion process is $t_d = (\delta\Gamma^S/DC^b)$). For a 6.2-$\mu$m-diameter bead with 10^6 receptors/bead, $\Gamma^S = 1.38 \times 10^{-10}$ mol/dm^2.

Least-squares error minimization[46] between this equation and experimental data was performed with a Nelder−Mead Simplex algorithm.[47] The fits to the experimental data yield the following parameter values: $K_d = 13.3 \pm 2.0$ nM, $k_f = (9.0 \pm 6.0) \times 10^4$ M^{-1} s^{-1}, $k_b = (1.2 \pm 0.8) \times 10^{-3}$ s^{-1}, and $D/\delta = (1.0 \pm 0.9) \times 10^{-9}$ dm s^{-1}, where the errors are the standard deviations for the constants determined from the fittings of each experimental run. Figure 3B shows the analysis of data corresponding to the end points in the egress of TR-M1 mAbs plugs through the affinity microcolumns. The equilibrium dissociation constant (K_d) from the binding curve is ∼10.0 nM,

(3) Flow Cytometry Equilibrium Binding Data. The equilibrium binding of TR-M1 to fluorescein-labeled FLAG peptides on beads is shown in Figure 4 as a sigmoidal response (binding) curve. The flow cytometer readings were taken after 30-min incubations of beads with TR-M1 mAbs. In comparison, the affinity microcolumn data were read after the injection of the 2-μL volume of mAbs (∼21 min). The flow cytometer intensity readings derive from the mean channel fluorescence[28,39] of bead-borne peptide fluorescence after binding of TR-M1 mAbs. The data are normalized to the intensity before quenching (via FRET) that occurs when the mAbs bind to the peptides on beads. The affinity

(46) Vijayendran, R. A.; Ligler, F. S.; Leckband, D. E. *Anal. Chem.* **1999**, *71*, 5405−5412.

(47) Lagarias, J. C.; Reeds, J. A.; Wright, M. H.; Wright, P. E. *SIAM J. Optimization* **1998**, *9*, 112−147.

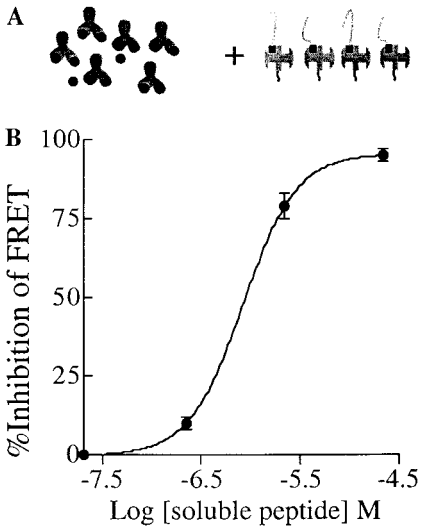

Figure 5. (A) Schematic representation of a competitive binding assay. TR-M1 mAbs are premixed with soluble and dark FLAG peptide (●), after which the sample is pumped through the affinity microcolumn comprosed of fluorescent FLAG peptide-bearing beads. The binding of the soluble peptide to TR-M1 mAbs is measured in terms of reduced FRET relative to neat TR-M1 samples. The initial concentration of TR-M1 mAbs (440nM) is in large excess of the peptides on beads (~25 nM). (B) Plot of percent inhibition of FRET versus concentration of soluble FLAG peptide. The extent of inhibition is dependent on stoichiometry. Some nonspecific binding is notable when [TR-M1] ≪ [soluble peptide].

constant was determined to be on the order of ~4.0 nM, which is comparable to that determined in the microcolumns.

(4) Competition. The analysis of 2-μL sample plugs with constant concentrations of TR-M1 mAbs (440.0 nM) mixed with varying concentrations of soluble, nonfluorescent FLAG peptide is shown in Figure 5. The concentrations of the soluble peptide span the range from 0 nM (not shown in the Figure) to $10^3 \times$ [TR-M1]. The increasing concentration of the dark peptide in each sample is manifested by the rise in the inhibition of FRET. The extent of FRET inhibition is consistent with the stoichiometric ratio between the TR-M1 mAbs and the soluble peptide. The blocking of FRET at the highest concentration of the soluble peptide is close to complete (>90%). Thus, the observed signal is attributed to nonspecific binding of the TR-M1, which is anticipated at the relatively high concentration of TR-M1.

DISCUSSION

We previously used a combination of flow cytometry and spectrofluorometry to analyze macromolecular interactions on the surfaces of microspheres.[28] The work was motivated by the need to develop bead-based methodologies for high-throughput proteomic[1] assays. We selected biotin (MW = 244.3) and a monoclonal antibody (MW ≈ 150 000) as prototypical analytes representative of small and large molecules, respectively. The equilibrium and kinetics of binding and dissociation of these two systems have been characterized and are reasonably well understood.[28,34,39,48,49] This enables us to make comparisons of data collected with flow cytometry and microcolumns. The presence of the analytes is monitored in real time by fluorescence intensity increases for detection of biotin and FRET for the detection of Texas Red-labeled monoclonal antibody.

A. Affinity Immunoassays. The approach to biomolecular assemblies displayed on microbead-based affinity columns has features in common with competitive binding immunoassays and affinity chromatography.[50−53] In these formats, a (fluorescently) tagged analyte analogue is incubated with a fixed amount of a dark target analyte and applied to a column that bears antibodies that can bind to both of these species. This is usually done by simultaneously or sequentially injecting the target analyte and its labeled analogue onto the column. The result is a method known as a chromatographic (or flow injection) immunoassay.[54−58] The generation of a signal is due to the presence of a target analyte in the sample that causes a change in the amount of labeled analyte that is able to bind to the antibodies in the system. A signal that corresponds to the target analyte's concentration is acquired by either measuring the amount of the labeled analyte that elutes in the nonretained peak or analyzing the bound labeled analyte that is released when an appropriate elution buffer is applied to the column. In the existing format, the beads bear fluorescent ligands/receptors of known surface occupancy. Thus, the subsequent changes from the initial intensity reading bear definite and known relationships to the amount of captured analytes, without contribution from unbound species. The direct analysis of the fate of the analyte species during passage through the affinity microcolumn may provide the best method for experimental verification of theoretical models of flow immunosensing.[46,59]

B. Sample Delivery in Microchannels: The Laminar Flow Regime. The flow of analyte fluid through the affinity microcolumns is laminar as is characterized by their low Reynolds numbers. The Reynolds number (*Re*) is a dimensionless parameter relating the ratio of inertial to viscous forces in a fluid.[12] Laminar flow is typical for $Re < 1$. For the current affinity microcolumns, we have estimated *Re* to be on the order of $\sim 1.0 \times 10^{-4}$.[60] There are several limiting practical considerations for sample delivery on this scale: viscous forces dominate over inertial forces and with the virtual loss of turbulence diffusion is the basic method of mixing of soluble reagents. The friction between the transporting fluid and the interstitial surface of the affinity microcolumn is manifested as a pressure drop (ΔP) across the microfluidic channel.[61−63] In bead-packed channels, the size of the beads and

(48) Chilkoti, A.; Stayton, P. S. *J. Am. Chem. Soc.* **1995**, *117*, 10622−10628.
(49) Jung, L. S.; Nelson, K. E.; Campbell, C. T.; Stayton, P. S.; Yee, S. S.; Perez-Luna, V. H.; Lopez, G. P. *Sens. Actuators, B* **1999**, *54*.
(50) Hage, D. S. *Clin. Chem.* **1999**, *45*, 593−615.
(51) Hage, D. S.; Thomas, D. H.; Chowdhuri, A. R.; Clarke, W. *Anal. Chem.* **1999**, *71*, 2965−2975.
(52) Hage, D. S.; Nelson, M. A. *Anal. Chem.* **2001**, *73*, 198A-205A.
(53) Clarke, W.; Chowdhuri, A. R.; Hage, D. S. *Anal. Chem.* **2001**, *73*, 2157−2164.
(54) Ruzicka, J. *Analyst* **1998**, *123*, 1617−1623.
(55) Ruzicka, J.; Scampavia, L. *Anal. Chem.* **1999**, *71*, A257−A263.
(56) Scampavia, L. D.; Hodder, P. S.; Lahdesmaki, I.; Ruzicka, J. *Trends Biotechnol.* **1999**, *17*, 443−447.
(57) Ruzicka, J. *Analyst* **2000**, *125*, 1053−1060.
(58) Ruzicka, J.; Hansen, E. H. *Anal. Chem.* **2000**, *72*, A212−A217.
(59) Holt, D. B.; Kusterbeck, A. W.; Ligler, F. S. *Anal. Biochem.* **2000**, *287*, 234−242.
(60) $Re = d_p U\rho/\mu$, where d_p is the diameter of the bead (6.2 μm), U is the velocity of the fluid through the microchannel ($\sim 2.5 \times 10^{-2}$ cms^{-1}), ρ is the density (~ 1 g/cm^3), and μ is the kinematic viscosity of the buffer ($\sim 10^{-2}$ cm^2 s^{-1}).
(61) Pfund, D.; Rector, D.; Shekarriz, A.; Popescu, A.; Welty, J. *AICHE J.* **2000**, *46*, 1496−1507.
(62) Seguin, D.; Montillet, A.; Comiti, J.; Huet, F. *Chem. Eng. Sci.* **1998**, *53*, 3897−3909.

length of the column play an essential role in regulating the magnitude of ΔP. For the affinity microcolumns of dimensions similar to those in Figure 1, empirical calculations have shown that the pressure drop across an empty channel is ~14 Torr while the affinity microcolumn sustains ΔPs on the order of 483 Torr for volumetric flow rates of 10 μL/min.[64]

C. Passage of Soluble Analytes through Affinity Microcolumns. (1) Fluorescein Biotin. The transport-limited kinetics and high affinity ($K_d \approx 10^{-13}$ M) of the binding of biotin to streptavidin[48] allows us to characterize the fluid flow properties inside the channel. The volume of the reactor vessel is composed of interstitial space between the receptor-bearing beads. The average time for a molecule to diffuse across a distance d, is $t = d^2/2D$, where D is the diffusion coefficient of the molecule ($D \approx 10^{-5}$ and 10^{-7}cm^2 s^{-1} for biotin and mAbs, respectively). In the column, d is small ($d \leq 1$ μm). The time lapse for diffusive contact between the ligand and receptor surface is correspondingly small (0.001−0.1 s depending on molecular weight). Because biotin is in large excess of the streptavidin receptors, the leading edge of the fluid passes through the column with negligible depletion of biotin. A direct correlation can therefore be made between the time-dependent increase in intensity and the velocity of the fluid. Based on the data in Figure 2B, the flow rate through the column (~4.0-nL interstitial volume) is on the order of 1.6 nL/s. Because the biotin experiment is essentially irreversible and quasi-unimolecular it serves as a useful standard for characterization of the affinity microcolumn and facilitates the analysis of the more complex antibody-binding data below.

(2) Analysis of Anti-FLAG Monoclonal Antibodies. The determination of the kinetic and equilibrium binding constants between ligand and receptor systems is fundamental to the understanding of biological function[65,66] as well as to the development of biomimetic systems.[2,26,67] From a mechanistic approach, the temporal and spatial destiny of target analytes (e.g., TR-M1) traversing through the affinity microcolumn might be described in terms of convective and diffusive transport and reactive (binding and dissociation) processes.[46,51,59] An additional point of detail in these analyses includes the generation of analyte concentration gradients[68,69] in the transport fluid as well as those bound on beads. Thus, a complete study of such phenomena would be very complex. The formalism used to analyze the interaction of TR-M1 mAbs and the peptides on beads (eqs 2 and 3) originates from the electrochemical literature,[45,70] where the model was used to examine the dynamics of molecular recognition between immobilized receptors and soluble analytes. This model reproduces the basic elements of mass transport-dependent heterogeneous kinetics. However, it does not account for the putative concentration gradients of bound species that are likely to emerge during passage of the TR-M1 mAbs through the affinity microcolumn. This simplifying assumption is possible because the microcolumn is smaller than the spot size of the laser beam used to irradiate the beads. The FRET-induced intensity changes associated with TR-M1/peptide complexes are integrated over the entire column. Thus, it is reasonable to make this simplified approach, with negligible loss of accuracy. The derived binding and dissociation rate constants ($k_f = (9.0 \pm 6.0) \times 10^4$ M s^{-1}, $k_b = (1.2 \pm 0.8) \times 10^{-3}$ s^{-1}) are in agreement with data reported in the literature on similar antibody−antigen interactions.[46,71] A gratifying validation of this approach is shown in the conservation of microscopic reversibility by the close correlation of the affinity constant derived from kinetic data ($K_d = k_b/k_f = 13.3$ nM) and that derived from steady-state data (~10.0 nM) shown in Figure 3.

Additional corroboration of the kinetic and equilibrium analyses of the affinity microcolumn data is shown in Figure 4. A sigmoidal dose−response curve of flow cytometry data using FLAG peptide-bearing beads and TR-M1 mAbs taken from the same preparation as the reagents used in the columns is shown.[39] The dissociation constants determined from flow cytometry (4.0 nM) and the affinity microcolumns (10.0 nM) are in good agreement. While the difference in the dissociation constants is within experimental error, it is worthy of comment. The binding of TR-M1 mAbs to the beads in the affinity microcolumn occurs under nonequilibrium conditions.[51,72] Thus, the binding of the mAbs is likely to be affected by mass transport limitations. Some evidence of this is shown by the shallow depth of the curve in Figure 3B relative to the curve that corresponds to the static flow cytometry assay in Figure 4.

E. Analytical Characteristics of the Affinity Microcolumn. In conventional affinity chromatography, resolving the kinetics of ligand−ligate binding is indirect, based on the analysis of the elution profile (retention times and peaks).[73] The system described here has the advantage of direct and real-time analysis and miniaturization. The high signal-to-noise ratio of these assays is due to the fact that the analytes are nonfluorescent (biotin) or do not contribute any background (TR-M1) to the change in the fluorescence of the fluorescein tag. The good correlation between kinetic and equilibrium data enables one to determine concentrations of analytes from dynamic response. Thus, assays could potentially be carried out in a few minutes, supplanting the need for time-consuming steady-state end point assays.

The analytical figures of merit (e.g., detection limit, dynamic range, sensitivity, and precision) for the immunoreaction are derived in Figure 3. The detection limit of the TR-M1 antibodies is in the subnanomolar range. Because of the tiny volumes allowed by the affinity microcolumn, it is useful to refer to the detection limits in terms of the minimal detectible amount of TR-M1, which for the 2-μL aliquot is on the order of femtomoles. In general, the linear dynamic range of an immunoassay is considered to span

(63) Seguin, D.; Montillet, A.; Comiti, J. *Chem. Eng. Sci.* **1998**, *53*, 3751−3761.
(64) We have estimated pressure exceeding 3 atm for volumetric flow rates of 50 μL/min from the Darcy equation for flow through packed beds (laminar flow, $Re < 1.0$): $\Delta P = [150\,\mu L v_s(1-e)^2]/[g_c D_p^2 \epsilon^3]$, where P is the pressure, μ the viscosity, L the length of the bed, v_s the superficial velocity, ϵ the void fraction, g_c the gravitational constant, and D_p the particle diameter. This is in contrast to a ΔP of 69 Torr across an empty channel. Our microcolumns could potentially withstand pressure drops of up to 2 atm before failing.
(65) Urry, D. W. *Angew. Chem., Int. Ed. Engl.* **1993**, *32*, 819−841.
(66) Alberts, B.; Bray, D.; Lewis, J.; Ratt, M.; Roberts, K.; Watson, J. D. *Molecular Biology of the Cell*, 2nd ed.; Garland: New York, 1989.
(67) Marvin, J. S.; Hellinga, H. W. *J. Am. Chem. Soc.* **1998**, *120*, 7−11.
(68) Jeon, N. L.; Dertinger, S. K. W.; Chiu, D. T.; Choi, I. S.; Stroock, A. D.; Whitesides, G. M. *Langmuir* **2000**, *16*, 8311−8316.
(69) Cabrera, C. R.; Finlayson, B.; Yager, P. *Anal. Chem.* **2001**, *73*, 658−666.
(70) Andrieux, C. P.; Saveant, J.-M. In *Investigation of Rates and Mechanisms of Reactions Part II*; Bernasconi, C. F., Ed.; Wiley: New York, 1986; Vol. VI, pp 305−390.
(71) Butler, J. E. In *Structure of Antigens*; Van Regenmortel, M. H. V., Ed.; CRC: Boca Raton, FL, 1992.
(72) Howard, M. E.; Holcombe, J. A. *Anal. Chem.* **2000**, *72*, 3927−3933.
(73) Leickt, L.; Mansson, A.; Ohlson, S. *Anal. Biochem.* **2001**, *291*, 102−108.

10−90% saturation of the antibody used (dashed horizontal lines in Figure 3B). This is usually equivalent to 2 orders of magnitude in analyte concentration (i.e., $0.1K_d$ < analyte <$10K_d$) in a conventional immunoassay[74] such as the flow cytometry assay shown in Figure 4. The data shown in Figure 3B, however, indicate a linear dynamic range spanning 4 orders of magnitude. The dynamic range in Figure 3B is extended on both the lower and upper limits in the concentration of the TR-M1 compared to Figure 4. A variety of mechanisms could explain the wider dynamic range apparent in Figure 3B. A possible factor that might extend the dynamic range is the heterogeneity in the affinity of the antibody for the peptide sites throughout the column. The binding of the antibodies to beads in the flow cytometric analysis is largely characterized by monovalent binding.[39] In the affinity column, the close packing of beads can allow (higher affinity) bivalent binding of the antibody, while transport effects[75] would tend to lower the monovalent affinity interactions. As a result, the dynamic range of the affinity microcolumn is extended in both directions, where the aggregate K_d remains comparable to the one that was determined with flow cytometry. On the basis of Figure 3B, the sensitivity of the affinity column appears to be linear throughout the dynamic range. The error bars shown in Figure 3B are representative of a minimum of three measurements, taken for each data point over an aggregate period of more than a month for the complete set of data replicates. All data points and replicates were measured in distinct affinity columns.

The specificity of the TR-M1/ FLAG peptide system on beads is very high. Coating the beads with bovine serum albumin (BSA) during assay preparation appears to eliminate nonspecific interactions for the antibody concentration within the useful dynamic range of this assay. At very high concentrations of TR-M1, nonspecific interactions may emerge. For example Figure 5 shows a competitive binding assay between bead-borne FLAG peptides and soluble nonfluorescent FLAG for the antibody binding sites. When the soluble peptide is a 1000-fold in excess of the TR-M1, negligible specific interaction is expected to occur with the bead-borne peptides; however, less than 10% of the FRET signal was observed. In a preliminary effort to establish the selectivity of this assay in a practical application, we have determined that the detection of TR-M1 and the FRET-blocking nonfluorescent peptide (cf. Figure 5) can be achieved in a controlled manner in an analyte fluid composed of blood serum and buffer.

SUMMARY AND CONCLUSIONS

This study has demonstrated some important factors related to the design, assessment, and utility of affinity microcolumn sensors. First, beads derivatized with surface chemistry suitable for the attachment of fluorescently labeled biomolecules of interest are prepared and characterized in terms of functionality and receptor site densities by flow cytometry. Second, calibrated beads are incorporated in microfluidic channels. The analytical device that emerges replicates the basic elements of affinity chromatography with the advantages of (1) scale, (2) direct measurement of bound analyte on beads rather than the indirect determination from eluted sample typical of affinity chromatography, and (3) simultaneous detection of multiple analytes from columns comprosed of discrete segments of diverse populations of receptor beads. We are currently developing a multianalyte model system comprosed of discrete segments of beads that bear distinct receptors for the simultaneous detection of diverse analytes. Since these assays consume very small sample volumes, multiple tests can be run, therefore saving on expensive reagents.

EXPERIMENTAL SECTION

Materials. The 6.2-μm-diameter streptavidin-coated polystyrene beads (Spherotech Inc., Libertyville, IL) were obtained as 0.5% (w/v) suspensions according to the manufacturer's data sheet. Hemocytometer analysis of the beads revealed the concentration of the particles to be in the range of $(4-5) \times 10^7$ beads/mL depending on the lot. Biotin, fluorescein biotin 5-((*N*-(5-(*N*-(6-(biotinoyl)amino)hexanoyl)amino)pentyl)thioureidyl)fluorescein), and (6-((6-((biotinyl)amino)hexanoyl)amino)hexanoic acid, succinimidyl ester (biotin-XX, SE) were purchased from Molecular Probes (Eugene, OR) and used without further purification. Anti-FLAG antibody was purchased from Sigma Chemical (St. Louis, MO). Biotinylated and fluoresceinated FLAG peptides (biotinyl-ϵ-aminocaproyl-KK(fluorescein)KDDDDKYD-NH_2, biotinyl-ϵ-amino caproyl-KKDDDDKYD-NH_2), and K(fluorescein)KDDDDKYD-NH_2) were synthesized at the University of New Mexico Protein Chemistry Laboratory.[39]

Texas Red Labeling of Anti-FLAG Monoclonal IgG. A 5-mg sample M1 IgG in 0.5 mL of sodium bicarbonate buffer was reacted with 50 μL of 1 mg/mL Texas-NHS (Molecular Probes) in DMSO for 2 h in the dark at room temperature. The antibody was freed of unreacted Texas-NHS by dialyzing the sample using minidialysis tubes (Pierce). It is noted that because Texas Red-labeled proteins tend to stick to chromatographic columns, the sample was purified and concentrated by ultrafiltration from phosphate-buffered saline using a 10 000 NMWCO Centricon membrane. The fluorophore to protein (f/p) ratios were determined following standard procedures from the manufacturers. The f/p ratios were generally on the order of 6:1.

Spectrofluorometry. Spectrofluorometric measurements were performed in single photon counting mode on an SLM-Aminco 8000 spectrofluorometer (SLM Instruments, Rochester, NY). The sample was excited at 490 nm, with a 10-nm band-pass interference filter (Corion Corp., Holliston, MA) used for line narrowing and stray light rejection. Fluorescein emission was monitored at 520 nm via a 520-nm (10 nm band-pass) filter (Corion Corp) and a long-pass band filter (3−70 Kopp Glass, Pittsburgh, PA). The latter filter is used to reduce stray excitation light**.** Neutral density filters were used to keep light intensities of the brightest samples within the dynamic range of the phototube.

Flow Cytometry. The flow cytometric analysis used a Becton-Dickinson FACScan flow cytometer (Sunnyvale, CA) interfaced to a Power PC Macintosh using the CellQuest software package. The FACScan is equipped with a 15-mW air-cooled argon ion laser. The laser output is fixed at 488 nm. It has been shown elsewhere[28] that the mean of the histogram is the quantity relevant to binding capacity. The average fluorescence of a single bead is converted to the number of fluorophores per bead on the basis of flow cytometric calibration beads.

(74) Andrade, J. D.; Lin, J. N.; Hlady, V.; Herron, J.; Christensen, D.; Kopecek, J. In *Biosensor Technology Fundamentals and Applications*, Buck, R. P., Hatfield, W. E., Umana, M., Bowden, E. F., Eds.; Marcel Dekker: New York, 1990; pp 219−239.

(75) Holt, D.; Rabbany, S. Y.; Kusterbeck, A. W.; Ligler, F. S. *Rev. Anal. Chem.* **1999**, *18*, 107−132.

Binding Analysis of Biotinylated Peptides to Streptavidin-Bearing Beads. Centrifugation Assays Using Paired Spectrofluorometric and Flow Cytometric Analysis. Experimental details of these analyses have been described elsewhere;[28,43] however, brief descriptions are provided for clarity. Centrifugation assays were used to determine the binding capacity of biotinylated fluorescent ligands to beads where the amount of bound ligand was determined from the fluorescence intensity of the residual supernatants using an SLM-Aminco 8000 spectrofluorometer. The resuspended beads were analyzed by flow cytometry using a Becton-Dickinson FACScan flow cytometer. We have shown elsewhere how molecular assemblies on beads can be analyzed in quantitative fashion by flow cytometry. The average fluorescence on a single bead is converted to the number of fluorophores per bead on the basis of flow cytometric calibration beads.[28,43] The affinity of biotinylated ligands for their receptor antibodies was determined in solution or on beads using FRET.[39]

Binding of TR-M1 mAbs to FLAG Peptide on Beads in Flow Cytometry. Detailed experimental procedure have been described elsewhere.[39] The 25-μL volumes of bead suspensions were added to microfuge tubes. Texas Red-labeled M1 was then added, in 1−2-μL volumes to obtain final concentrations ranging from 1.0 to 300.0 nM in the respective tubes. The samples were incubated for 30 min with shaking. The samples were then transferred to FACScan tubes, and buffer was added to a final volume of 200 μL for flow cytometry analysis of mean channel fluorescence, which reflects the extent of the energy transfer between peptide and TR-M1 due to increasing [TR-M1] mAbs. The change in intensity with each addition of antibody was monitored continuously until the end point was reached.

Preparation of Microchannels. The microfluidic channels were made from an elastomeric polymer, PDMS, following published methods[40,41] employing standard photolithographic techniques. A prototypical microfluidic channel (as shown in Figure 1A) was 3 cm long, with typical dimensions of 250 μm by 50 μm, respectively, in breadth and depth, patterned into a PDMS elastomer adhered to a glass slide support. Within the microchannel, obstructive features, 20 μm apart are patterned as filters to hold 30-μm beads. A plug of cotton can be used as an alternative filter to hold the beads.

Packing of Microchannels with Beads. In a typical experiment, a 30-μL aliquot suspension of 30-μm beads ($\sim 10^6$ beads/mL) was injected into the channel with a Hamilton syringe. A peristaltic pump connected to the ("waste" port in Figure 1A) channel was used to remove the supernatant. A foundation layer of 30-μm beads was used to hold subsequent layers of smaller beads. The contents were allowed to settle during the peristaltic pump-assisted elution of several microliters of buffer. To minimize the dispersion of the 6.2-μm streptavidin-coated beads into the foundation layer of 30−μm beads, a layer of 10−μm glass beads was added to the microchannel as described above. Subsequently, 6.2-μm ligand-bearing polystyrene beads ($\sim 1.0 \times 10^6$ beads/mL or $\sim$30 000 beads in the microchannel) were added to the microchannel in Tris buffer (pH 7.5) containing 0.1% BSA. Several microliters of the buffer were eluted through the column, coating the PDMS microchannel with BSA. The coating minimized the potential for nonspecific adsorption of protein and peptides to the walls of the microchannels in subsequent assays. Once packed, the column was ready to use. In this work, we used streptavidin-coated beads displaying known quantities of either fluorescein biotin or fluorescent FLAG peptide. Their respective "analytes", native biotin or Texas Red-tagged anti FLAG antibodies, were injected into the channel in 2-μL aliquots. The time course of the interaction between the analyte solutions and beads was monitored on a Model Fluorolog-3 SPEX fluorometer (Instruments S.A., Edison NJ) using 488-nm laser excitation focused onto the 0.6-mm-long portion of the column containing the fluorophore-bearing beads.

Fluorescein Biotin Column. Streptavidin-coated beads bearing $\sim 1 \times 10^6$ fluorophores/bead were packed into the microchannel (vide supra). The analyte fluid (3.0 mM biotin in 2 μL) was added to the column and monitored as increasing emission intensity of the beads as the fluid flowed through the column.

Fluorescent FLAG Peptide-Bearing Beads. Several affinity microcolumns were prepared using $\sim 1.0 \times 10^6$ peptides/bead.[39] Two-microliter plugs of Texas Red-labeled M1 anti-FLAG monoclonal antibodies were eluted at varying concentrations in different affinity microcolumns. The binding of the antibody to the FLAG peptide was monitored as quenching of the peptide emission. To ensure the specificity of the binding of TR-M1 mAbs to beads, samples of the mAbs were preequilibrated with varying amounts of a dark (nonfluorescent peptide) FLAG peptide and passed through the microcolumns.

ACKNOWLEDGMENT

This work was supported by the Department of Defense through the Multidisciplinary Research Program of the University Research Initiative (Office of Naval Research) Grant N00014-95-1-1315, National Science Foundation (MCB-9907611) (to T.B.), NIH-BECON (GM60799-02), Air Force Office of Scientific Research N00014-95-1, NIH RR-01315 to the National Flow Cytometry Resource, and NM State Cigarette tax to the UNM Cancer Center.

Received for review August 29, 2001. Accepted December 11, 2001.

AC0109624